onlinelibrary.wiley.com/doi/10.1002/zaac.202200066 by University Of California, Riverside, Wiley Online Library on [30/1/22022]. See the Terms and Conditions (https://doi.org/10.1001/2002).

litions) on Wiley Online Library for rules of use; OA articles are governed by the applicable Creative Commons

DOI: 10.1002/zaac.202200066

# Fe<sub>5</sub>Ge<sub>2</sub>Te<sub>2</sub>: Iron-rich Layered Chalcogenide for Highly Efficient Hydrogen Evolution

Eunsoo Lee<sup>+</sup>,<sup>[b]</sup> Amir A. Rezaie<sup>+</sup>,<sup>[a]</sup> Diana Luong<sup>+</sup>,<sup>[c]</sup> Johan A. Yapo<sup>+</sup>,<sup>[c]</sup> and Boniface P. T. Fokwa<sup>\*[a, c]</sup>

Dedicated to Professor Mercouri Kanatzidis on the occasion of his 65th birthday

Recent research on van der Waals (vdW) metal chalcogenides electrocatalysts for the hydrogen evolution reaction (HER) has been devoted to finding new catalysts with active basal planes. Here, we report on experimental and theoretical investigations of the HER activity of a recently discovered iron-rich vdW spintronic material, Fe<sub>3</sub>Ge<sub>2</sub>Te<sub>2</sub> (FG2T) in alkaline media (1 M KOH). We show that a densified electrode of FG2T requires an overpotential of only -90.5 mV to drive a current density of 10 mA/cm<sup>2</sup>. Free energy calculations of hydrogen adsorption using density functional theory (DFT) proved that the numerous

sites present on the hexagonal Te layer are more active than those found in the recently proposed Fe<sub>3</sub>GeTe<sub>2</sub> (FGT) catalyst, supporting higher activity for the new Fe-richer catalyst. Like in FGT, XPS analysis has found that a thin oxide layer covers the active FG2T layers, suggesting the real active surface to be a hybrid FG2T/oxide layer. These results strengthen the idea of continued screening of iron-based vdW materials to replace the non-abundant platinum group electrocatalysts toward HER and other electrocatalytic processes.

Recent climate change-related issues and the increase in energy demand are helping to accelerate the transition from nonrenewable and polluting fuels such as fossil fuels and coal to renewable and non-toxic ones.[1] Due to its cleanliness, sustainability and high energy density hydrogen has been accepted as one of the most promising, eco-friendly alternatives. [2] Furthermore, hydrogen can be produced through water electrolysis, which is an environmental-friendly method. [3] Many research efforts in this field are focused on developing new, efficient, and cost-effective electrocatalysts to replace current scarce and expensive platinum-group metals and noble-metal compounds.[4]

Van der Waals (vdW) materials such as transition metal dichalcogenides (TMDs) are among the most-studied HER electrocatalysts due to their unique physical and chemical properties. The majority of these vdW materials do not show basal plane electrochemical activity toward HER, making them almost inactive in bulk form. Therefore, to improve the basal plane activity, various surface modifications such as defect

engineering, [6] doping, [7] and interfacial engineering [8] have been successfully applied. Recent research is focused on the development of new basal-plane-active vdW materials that will induce greater electrochemical activity post surface modifications. Among all the vdW layered materials, some are being considered for spintronic applications, especially Fe<sub>3-x</sub>GeTe<sub>2</sub> (FGT), which is an itinerant ferromagnet below a Curie temperature of 220 K.[9] Similar to other TMDs, FGT is currently being considered as a potential electrocatalyst candidate for several reactions, including the oxygen-evolution reaction (OER) and nitrogen reduction reaction (NRR). [5d,10] We have recently reported the first experimental and theoretical investigations of the HER activity of FGT.[11] We found that a densified FGT electrode requires the smallest overpotential ( $\eta_{10} = -0.105 \text{ V}$ ) among all bulk TMDs reported so far, and that it displays no significant HER activity loss after 3000 cycles and 24 hours of operation in an alkaline electrolyte. Furthermore, density functional theory (DFT) calculations of the free energy of hydrogen adsorption ( $\Delta G_H$ ) showed that FGT's flat Te basal plane is as active as the puckered Te layer in monoclinic MoTe<sub>2</sub> (1T'-MoTe<sub>2</sub>),<sup>[12]</sup> thus supporting the basal plane activity of FGT. All active basal plane TMDs so far have puckered chalcogenide basal planes including 3R-MoS<sub>2</sub>, [13] making FGT the first electrocatalyst with an active flat basal plane. Additionally, DFT calculations presented an active edge layer (106) that is superior to the basal plane, supporting the observed increased activity with particle size reduction. The discovery of FGT's HER activity has put other iron-based vdW materials into focus, especially those richer in iron as they will ultimately be less expensive than FGT. Herein, we report on the experimental and theoretical investigations of the HER activity of a recently discovered ironricher phase that is structurally related to FGT, Fe<sub>5-x</sub>Ge<sub>2</sub>Te<sub>2</sub> (FG2T). Compared to FGT, FG2T has an extra Fe<sub>2</sub>Ge layer that

[a] A. A. Rezaie, \* B. P. T. Fokwa

Materials Science and Engineering, University of California, Riverside, CA-92521, USA

E-mail: bfokwa@ucr.edu

Homepage: https://fokwalab.ucr.edu/

[b] E. Lee

Department of Chemical and Environmental Engineering, University of California, Riverside, CA-92521, USA

- [c] D. Luong, J. A. Yapo, B. P. T. Fokwa Department of Chemistry and Center for Catalysis, University of California, Riverside, CA-92521, USA
- [+] co-first authors
- Supporting information for this article is available on the WWW under https://doi.org/10.1002/zaac.202200066

allows for a change in crystal symmetry from a hexagonal (space group  $P\bar{6}_3/mmc$ ) to trigonal (space group  $P\bar{3}m1$ ). In fact, FG2T's crystal structure consists of a "Fe<sub>5-x</sub>Ge<sub>2</sub>" substructure sandwiched between two layers of Te atoms weakly bonded by vdW forces on adjacent slabs as seen in Figure 1c.

The FG2T sample was synthesized via our previous method<sup>[14]</sup> through a solid-state reaction [check the SI for details]. The as-grown crystals were characterized by powder X-ray diffraction (PXRD) for their phase purity (Figure 1a), scanning electron microscope (SEM) for their morphology, and energy dispersive X-ray spectroscopy (EDS) mapping (Figure 1b) for elemental distribution. The PXRD pattern displayed FG2T as the majority phase (90%), according to Rietveld refinement (Figure S1). However small percentages of FGT (8.3%) and Fe<sub>2-x</sub>Ge (1.7%) were identified as side phases. Intensity mismatches were also observed for the (*00I*) peaks, similar to the previously reported FGT,<sup>[11]</sup> which is due to the preferred orientation of these layered crystals (Figure 1b). The EDS mapping on the FG2T crystals confirmed the existence and homogenous distribution of all three elements (Figure 1b).

In our previous report on the HER activity of FGT,<sup>[11]</sup> we showed that a pressed pellet electrode from an ultrasonicated powder sample of this vdW material has the best performance versus its bulk or sonicated powder electrode forms. Therefore, we have studied the HER activity of FG2T based on its similarly pressed pellet electrode. FG2T powder was dispersed in ethanol and ultrasonicated in an ice-water bath for two hours. The ultrasonicated powder was then compressed under a hydraulic press at room temperature

providing a densified disk (check the SI for more details). The PXRD pattern of the densified pellet displayed an increased preferred orientation toward the [00l] direction similar to the previously reported FGT (Figure 1a). The preferred orientation was also observed for the small FGT impurity. SEM micrograph confirmed the highly oriented sheet-like morphology of the electrode's surface (Figure S2).

X-ray photoelectron spectroscopy (XPS) was applied to investigate the surface chemical composition and the corelevel binding energy of the FG2T pellet before (Figure 2) and after HER activity measurements (Figure S3). The results of the analyzed surface show the oxidation states of the Fe 2p, Ge 3d, and Te 3d species (Figure 2 and Table S1). As seen in Figure 2a, the spectra are very similar to those reported for FGT,[11,15] thus only similarities and differences will be discussed here. Similar to FGT, the high-resolution Fe 2p spectrum shows two peaks at 706.6 eV/719.6 eV which originate from the metallic iron (Fe<sup>0</sup> in FG2T) as well as two other doublets at 710.9 eV and 724.5 eV (with 713.2 and 726.2 eV satellites)[11,15] ascribed to Fe<sup>3+</sup> from the surface oxide layer. The highresolution Ge 3d spectrum (Figure 2b) depicts peaks at 29.2/ 29.9 eV assigned to metallic germanium (Ge<sup>0</sup> in FG2T) and others at 31.7 eV (Ge<sup>2+</sup>) and 32.5 eV (Ge<sup>4+</sup>) corresponding to germanium oxide peaks.[11,16] The high-resolution Te 3d spectrum (Figure 2c) contains peaks at 573.2/583.5 eV ascribed to metallic tellurium (Te<sup>0</sup> in FG2T) while those at 576.5/ 586.9 eV are assigned to Te<sup>4+</sup>.[11,17] The O 1s spectrum (Figure 2d) indicates peaks at 530.6 eV and 532.4 eV assigned to metal oxide and oxygen deficiencies on the surface, respectively.[18] The sonication decreases the particle size, thus

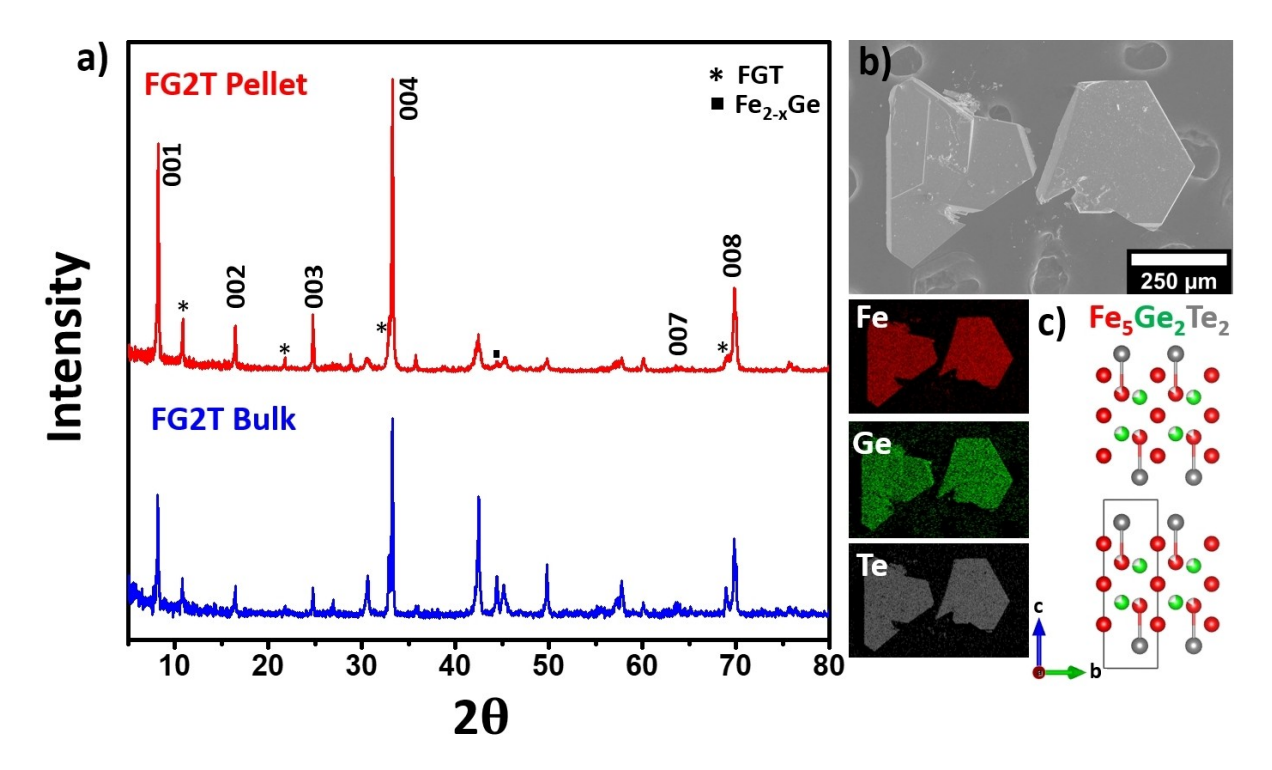


Figure 1. a) Powder X-ray diffraction patterns of FG2T samples (bulk and pellet). b) SEM images and EDS mappings of as-synthesized FGT crystals. c) Crystal structure of FG2T (\* represents FGT peaks,  $\blacksquare$  represents Fe<sub>2-x</sub>Ge peaks)

library.wiley.com/doi/10.1002/zaac.202200066 by University Of California

, Riverside, Wiley Online Library on [30/12/2022]. See

on Wiley Online Library for rules of use; OA articles are governed by the applicable Creative Comm

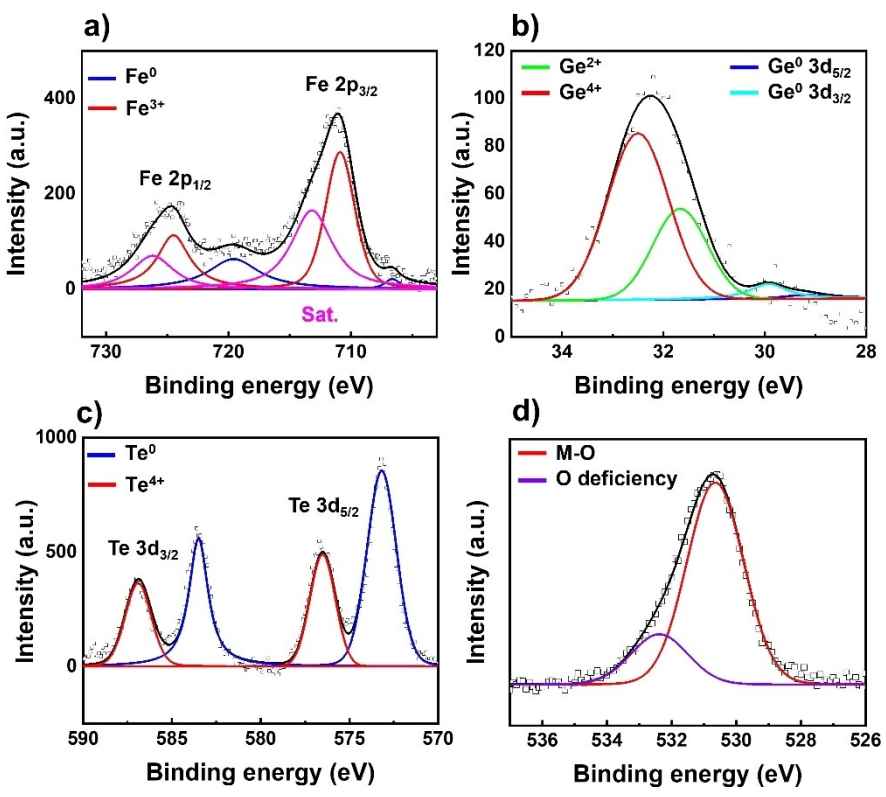


Figure 2. X-ray photoelectron spectroscopy spectra of a) Fe 2p, b) Ge 3d, c) Te 3d, and d) O 1s for the sonicated FG2T pellet. Experimental and fitting data are indicated as ( $\square$ ) and solid lines, respectively.

exposing more surface area to oxidation. However, the FG2T peaks are still clearly detectable by XPS, suggesting that the formed oxide layer is thin. In fact, the peak intensities of Te<sup>0</sup> are higher than those of the oxidized Te-species, indicating that Te<sup>0</sup> is the most abundant species on the surface due to the Te-terminated vdW atomic structure in FG2T. This finding contrasts with that of FGT which showed dominating oxidized Te-species instead. Interestingly, our DFT calculations (discussed later in the manuscript) clearly show that FG2T is intrinsically active, showing even more active sites on its basal Te plane than FGT. Nevertheless, the presence of surface oxidized species may affect the HER activity, suggesting that the real active surface may be a complex hybrid FG2T/oxide layer.

The HER activity of the FG2T pellet electrode was examined in 1 M KOH electrolyte. To rule out any effect of the Fe<sub>2-x</sub>Ge impurity, its activity was studied, and it showed very poor performance (Figure S4). The linear sweep voltammetry (LSV) curve of the sonicated FG2T pellet exhibits an overpotential of  $\eta_{10} = -90.5$  mV at  $10 \text{ mA/cm}^2$  and  $\eta_{250} = -358$  mV at a high current density of  $250 \text{ mA/cm}^2$  (Figure 3a). Consequently, the FG2T pellet shows a 13.8% improved overpotential (at  $10 \text{ mA/cm}^2$ ) if compared to the previously reported FGT pellet ( $\eta_{10} = -105 \text{ mV}$  and  $\eta_{250} = -398 \text{ mV}$ ). To support this result, we have estimated the electrochemical active surface area (ECSA) from cyclic voltammetry (CV) measured at various scan rates. ECSA was estimated from the

electrochemical double-layer capacitance (C<sub>dl</sub>). The C<sub>dl</sub> is linearly proportional to the effective surface area. This is because the double layer charging current (i<sub>c</sub>) is proportional to the electrochemically active surface area of the electrode. [19] Therefore, large C<sub>dl</sub> indicates more exposed surface-active sites. Figure S5 shows that the C<sub>dl</sub> value (55.2 mF/cm<sup>2</sup>) of the FG2T pellet is larger than that reported for the FGT pellet (52.7 mF/cm<sup>2</sup>), [11] confirming the presence of more active sites on FG2T. Furthermore, electrochemical impedance spectroscopy (EIS) data in Figure S6 and Table S2 also indicate that FG2T is a more efficient electrocatalyst than FGT. The first parallel components (R<sub>ct</sub> and CPE) indicate the charge transfer kinetics and the second parallel components (R and C) reflect the hydrogen adsorption behavior. [20] In fact, the charge transfer resistance (R<sub>ct</sub>), which is derived from the Nyquist plot, shows that the FG2T electrode has a smaller R<sub>ct</sub>  $(8.06 \Omega)$  than the FGT electrode  $(9.71 \Omega)_{t}^{[11]}$  supporting the idea that electrons will move more efficiently on the FG2T electrode surface and thus boosting its charge transfer rate during HER.

The Tafel slope was used to understand the reaction kinetics by evaluating the rate-determining step. From the Tafel plots (Figure 3b) extracted from the LSV curve, the FG2T pellet demonstrates a high HER activity with a lower Tafel slope (93.4 mV/dec) versus the FGT pellet electrodes (97.3 mV/dec), indicating a more efficient HER with faster kinetics for FG2T. In the

loi/10.1002/zaac.202200066 by University Of California, Riverside, Wiley Online Library on [30/12/2022]. See the Terms

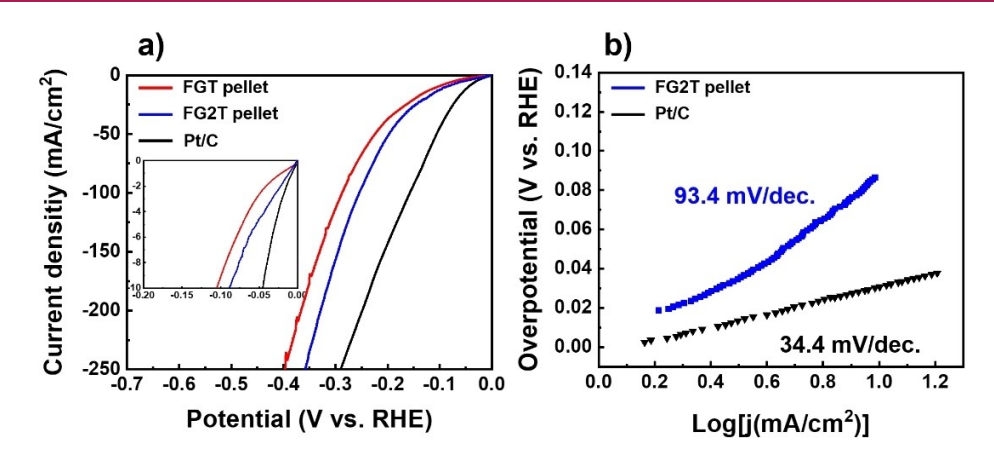


Figure 3. a) Polarization curves of sonicated FG2T pellet, sonicated FGT pellet from the previous study, [11] and Pt/C. The data was recorded in 1 M KOH at a scan rate of 1 mV/s with iR-correction. b) Tafel plots obtained using the polarization curves in a).

alkaline electrolyte, there are three microscopic steps as shown below.[21]

Tafel reaction:

$$2 H_{ad} \hookrightarrow H_2$$
 (Tafel slop =  $\sim 30 \text{ mV/dec}$ )

Heyrovsky reaction:

$$H_{ad} + e^- + H_2O \Longrightarrow H_2 + OH^-$$
 (Tafel slop =  $\sim 40 \text{ mV/dec}$ )

Volmer reaction:

$$H_{ad} + OH^- \Leftrightarrow H_2O + e^-$$
 (Tafel slop =  $\sim 120 \text{ mV/dec}$ )

The FG2T pellet's Tafel slope is located between that proposed for the Volmer reaction (Tafel slope  $\sim 120 \text{ mV/dec}$ ) and that of the Heyrovsky reaction (Tafel slope  $\sim 40 \text{ mV/dec}$ ), hinting at a complex reaction as often observed for highly

active bulk catalysts. [22] Moreover, continuous CV measurements were used to evaluate the stability of FG2T (Figure S7a), and the electrode showed very little degradation after 3000 cycles. Besides, at a fixed overpotential, a chronoamperometric test (Figure S7b) of the electrode yields a stable current density of about 10 mA/cm² for 24 h, proving its high durability under these HER conditions. The high stability of the FG2T electrode was further confirmed by XPS, which showed almost identical spectra before (Figure 2) and after (Figure S3) HER activity measurements. In the O 1s spectrum, a hydroxide peak appears after electrochemical measurement due to the alkaline electrolyte. However, the amount is so small that it did not affect the activity.

According to the XPS results discussed above Te<sup>0</sup> from the FG2T basal plane is the dominant species on the FG2T's surface and electrochemical activity studies proved that FG2T is more active than FGT. Consequently, we hypothesized that FG2T should have a more active Te basal plane than FGT. To verify

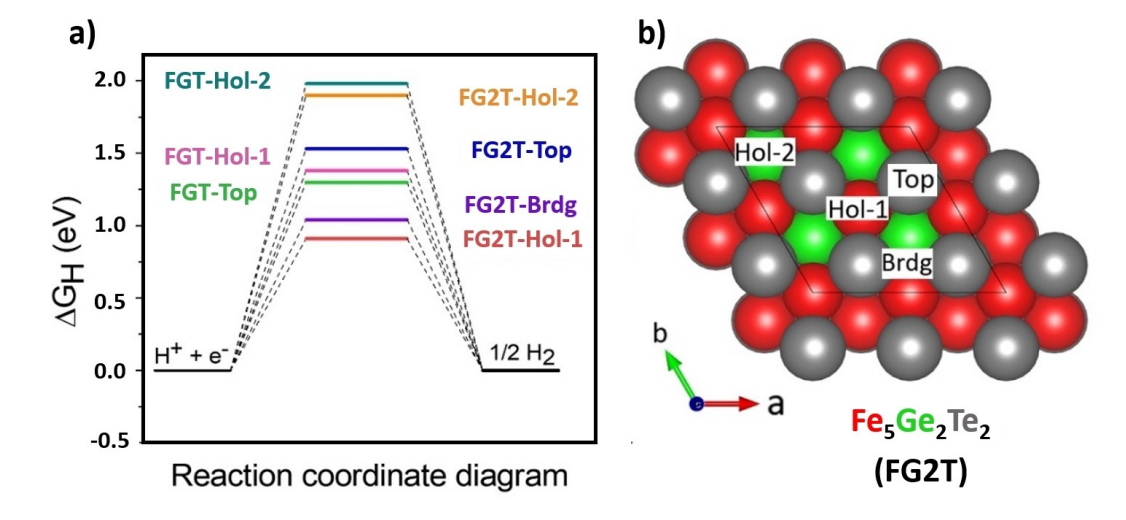


Figure 4. a) The Gibbs free energy ( $\Delta G_H$ ) of H-adsorption on the studied active sites of FG2T and FGT (obtained from [11]). b) FG2T slab model generated for the (002) basal plane highlighting the studied sites.

this hypothesis first-principles DFT calculations were carried out on a model of FG2T's basal plane (002) using a unit cell doubled in the c-direction. The Gibbs free energy ( $\Delta G_H$ ) values of different H-adsorption sites were calculated.  $\Delta G_H$  for atomic hydrogen adsorbing on a catalyst surface is widely accepted as a descriptor of HER activity as it was shown to correlate with the experimentally measured HER activity for a variety of systems. [23] Theoretically, the optimal HER activity is achieved when the  $\Delta G_H$  value is close to zero, as it ensures that the reaction rates for both a H atom adsorbing and H2 molecule desorbing onto/off the surface are maximized. For the alltellurium (002) layer, four sites were considered as shown in Figure 4b: (1) on top (Top) of a Te atom, two hollow sites (2&3), one above an Fe atom (Hol-1) and another above a Ge atom (Hol-2), and lastly (4) a bridge (Brdg) site between two Te atoms. The calculated  $\Delta G_H$  values are 1.53 eV, 0.91 eV, 1.90 eV, and 1.04 eV for the Top, Hol-1, Hol-2, and Brdg sites, respectively. As Figure 4a illustrates, almost all sites are also present in the recently discovered HER-active FGT, with the missing site in FGT being the bridge site which converged to the top site after structure optimization.[11] Interestingly, comparing the  $\Delta G_H$  values of the two materials (Figure 4a) shows that the FG2T-Brdg site is more active than the best FGT site (Top). Furthermore, the two most active FG2T sites (Hol-1 and Brdg) have lower  $\Delta G_H$  than all FGT sites. These theoretical results not only supports the experimental findings that FG2T is more HER active than FGT, but it also possesses a basal plane that is more active than other highly studied chalcogenides such as 1T'-MoTe<sub>2</sub><sup>[24]</sup> and 3R-MoS<sub>2</sub>.<sup>[13]</sup>

In summary, the iron-rich layered chalcogenide Fe<sub>5-x</sub>Ge<sub>2</sub>Te<sub>2</sub> (FG2T) was synthesized by a solid-state reaction route and characterized through PXRD, SEM, and EDS analyses. The HER activity of the FG2T pellet was investigated, the results of which demonstrated an improved HER activity by 13.8% if compared to the recently reported iron-poorer Fe<sub>3-x</sub>GeTe<sub>2</sub> (FGT) pellet. DFT calculations evaluated and confirmed these findings by discovering the existence of numerous active sites on the hexagonal tellurium layer of FG2T, two of which attained lower  $\Delta G_{\rm H}$  values versus all FGT sites. This study introduces FG2T as a highly HER active trigonal vdW material showing the most active basal plane to date among all vdW materials.

### Acknowledgments

This work was supported by the startup fund to BPTF at UC Riverside and a partial support from the National Science Foundation Career award to BPTF (no. DMR-1654780). The San Diego Supercomputer Center (SDSC) is gratefully acknowledged for providing computing resources. The XPS data were collected with an instrument acquired through the NSF MRI program (DMR-0958796).

#### **Conflict of Interest**

The authors declare no conflict of interest.

#### **Data Availability Statement**

The data that support the findings of this study are available on request from the corresponding author. The data are not publicly available due to privacy or ethical restrictions.

**Keywords:** Van der Waals (vdW) materials  $\cdot$  Fe<sub>5</sub>Ge<sub>2</sub>Te<sub>2</sub> (FG2T)  $\cdot$  Electrocatalysts  $\cdot$  Hydrogen evolution  $\cdot$  DFT calculations.

- [1] a) J. Chow, R. J. Kopp, P. R. Portney, *Science* **2003**, *302*, 1528–1531; b) I. Roger, M. A. Shipman, M. D. Symes, *Nat. Chem. Rev.* **2017**, *1*, 0003.
- [2] a) J. A. Turner, Science 2004, 305, 972–974; b) F. Bonaccorso, L. Colombo, G. Yu, M. Stoller, V. Tozzini, A. C. Ferrari, R. S. Ruoff, V. Pellegrini, Science 2015, 347, 1246501; c) Z. Xie, P. He, L. Du, F. Dong, K. Dai, T. Zhang, Electrochim. Acta 2013, 88, 390–394.
- [3] a) C. C. McCrory, S. Jung, I. M. Ferrer, S. M. Chatman, J. C. Peters, T. F. Jaramillo, J. Am. Chem. Soc. 2015, 137, 4347–4357;
  b) N. S. Lewis, D. G. Nocera, Proc. Natl. Acad. Sci. USA 2006, 103, 15729–15735;
  c) T. R. Cook, D. K. Dogutan, S. Y. Reece, Y. Surendranath, T. S. Teets, D. G. Nocera, Chem. Rev. 2010, 110, 6474–6502.
- [4] a) S. Park, Y. Shao, J. Liu, Y. Wang, Energy Environ. Sci. 2012, 5,
   9331–9344; b) J. Feng, F. Lv, W. Zhang, P. Li, K. Wang, C. Yang,
   B. Wang, Y. Yang, J. Zhou, F. Lin, Adv. Mater. 2017, 29, 1703798.
- [5] a) H. Li, C. Tsai, A. L. Koh, L. Cai, A. W. Contryman, A. H. Fragapane, J. Zhao, H. S. Han, H. C. Manoharan, F. Abild-Pedersen, *Nat. Mater.* 2016, 15, 48–53; b) D. Voiry, R. Fullon, J. Yang, C. d. C. C. e Silva, R. Kappera, I. Bozkurt, D. Kaplan, M. J. Lagos, P. E. Batson, G. Gupta, *Nat. Mater.* 2016, 15, 1003–1009; c) Y. Wang, Y. Li, T. Heine, *J. Am. Chem. Soc.* 2018, 140, 12732–12735; d) Y. Zhao, J. Gu, Z. Chen, *Adv. Funct. Mater.* 2019, 29, 1904782.
- [6] a) D. Li, Y. Jia, G. Chang, J. Chen, H. Liu, J. Wang, Y. Hu, Y. Xia, D. Yang, X. Yao, Chem 2018, 4, 2345–2356; b) Y. Li, K. Yin, L. Wang, X. Lu, Y. Zhang, Y. Liu, D. Yan, Y. Song, S. Luo, Appl. Catal. B 2018, 239, 537–544; c) G. Ou, P. Fan, X. Ke, Y. Xu, K. Huang, H. Wei, W. Yu, H. Zhang, M. Zhong, H. Wu, Nano Res. 2018, 11, 751–761.
- [7] a) Y. Qin, H.-H. Wu, L. A. Zhang, X. Zhou, Y. Bu, W. Zhang, F. Chu, Y. Li, Y. Kong, Q. Zhang, ACS Catal. 2018, 9, 610–619; b) Z. Luo, Y. Ouyang, H. Zhang, M. Xiao, J. Ge, Z. Jiang, J. Wang, D. Tang, X. Cao, C. Liu, Nat. Commun. 2018, 9, 1–8; c) Y. Zhao, J. Wan, H. Yao, L. Zhang, K. Lin, L. Wang, N. Yang, D. Liu, L. Song, J. Zhu, Nat. Chem. 2018, 10, 924–931.
- [8] a) Z. Zhu, H. Yin, C. T. He, M. Al-Mamun, P. Liu, L. Jiang, Y. Zhao, Y. Wang, H. G. Yang, Z. Tang, Adv. Mater. 2018, 30, 1801171; b) M.-R. Gao, J.-X. Liang, Y.-R. Zheng, Y.-F. Xu, J. Jiang, Q. Gao, J. Li, S.-H. Yu, Nat. Commun. 2015, 6, 1–7; c) H. Hong, C. Liu, T. Cao, C. Jin, S. Wang, F. Wang, K. Liu, Adv. Mater. Interfaces 2017, 4, 1601054.
- [9] a) N. K. Abrikosov, L. Bagaeva, L. Dudkin, *Izv. Akad. Nauk SSSR Neorg. Mater.* 1985, 21, 1680–1686; b) H. J. Deiseroth, K. Aleksandrov, C. Reiner, L. Kienle, R. K. Kremer, *Eur. J. Inorg. Chem.* 2006, 2006, 1561–1567.
- [10] a) Z. Cui, C. Xiao, Y. Lv, Q. Li, R. Sa, Z. Ma, Appl. Surf. Sci. 2020, 527, 146894; b) Z. Ma, C. Xiao, Z. Cui, W. Du, Q. Li, R. Sa, C. Sun, J. Mater. Chem. A 2021, 9, 6945–6954.
- [11] A. A. Rezaie, E. Lee, D. Luong, J. A. Yapo, B. P. Fokwa, ACS Materials Lett. 2021, 3, 313–319.
- [12] J. C. McGlynn, I. Cascallana-Matías, J. P. Fraser, I. Roger, J. McAllister, H. N. Miras, M. D. Symes, A. Y. Ganin, *Energy Technol.* 2018, 6, 345–350.

## RESEARCH ARTICLE

ed from https://onlinelibrary.wiley.com/doi/10.1002/zaac.202200066 by University Of California, Riverside, Wiley Online Library on [30/12/2022]. See

of use; OA articles are governed by the applicable Creative Cor

- [13] R. J. Toh, Z. Sofer, J. Luxa, D. Sedmidubský, M. Pumera, Chem. Commun. 2017, 53, 3054–3057.
- [14] P. R. Jothi, J. P. Scheifers, Y. Zhang, M. Alghamdi, D. Stekovic, M. E. Itkis, J. Shi, B. P. Fokwa, *Phys. Status Solidi RRL* 2020, 14, 1900666
- [15] a) Y. Yan, B. Y. Xia, X. Ge, Z. Liu, A. Fisher, X. Wang, Chem. Eur. J. 2015, 21, 18062–18067; b) A. P. Grosvenor, S. D. Wik, R. G. Cavell, A. Mar, Inorg. Chem. 2005, 44, 8988–8998; c) H. Li, P. Wen, Q. Li, C. Dun, J. Xing, C. Lu, S. Adhikari, L. Jiang, D. L. Carroll, S. M. Geyer, Adv. Energy Mater. 2017, 7, 1700513; d) R. Liang, L. Shen, F. Jing, N. Qin, L. Wu, ACS Appl. Mater. Interfaces 2015, 7, 9507–9515.
- [16] a) V. Grossi, L. Ottaviano, S. Santucci, M. Passacantando, J. Non-Cryst. Solids 2010, 356, 1988–1993; b) Y. Huang, J.-P. Xu, L. Liu, P.-T. Lai, W.-M. Tang, IEEE Trans. Electron Devices 2016, 63, 2838–2843; c) Q. Xie, S. Deng, M. Schaekers, D. Lin, M. Caymax, A. Delabie, X.-P. Qu, Y.-L. Jiang, D. Deduytsche, C. Detavernier, Semicond. Sci. Technol. 2012, 27, 074012.
- [17] a) Z. Yang, M. Xu, X. Cheng, H. Tong, X. Miao, Sci. Rep. 2017, 7,
   1–9; b) M. O. Reese, C. L. Perkins, J. M. Burst, S. Farrell, T. M. Barnes, S. W. Johnston, D. Kuciauskas, T. A. Gessert, W. K. Metzger, J. Appl. Phys. 2015, 118, 155305.
- [18] a) M. M. Sabri, J. Jung, D. H. Yoon, S. Yoon, Y. J. Tak, H. J. Kim, J. Mater. Chem. C 2015, 3, 7499–7505; b) F. Liu, C. Chen, H. Guo,

- M. Saghayezhian, G. Wang, L. Chen, W. Chen, J. Zhang, E. Plummer, *Surf. Sci.* **2017**, *655*, 25–30.
- [19] a) S. Trasatti, O. Petrii, Pure Appl. Chem. 1991, 63, 711–734;
   b) J. D. Benck, Z. Chen, L. Y. Kuritzky, A. J. Forman, T. F. Jaramillo, ACS Catal. 2012, 2, 1916–1923.
- [20] J. Li, H.-X. Liu, W. Gou, M. Zhang, Z. Xia, S. Zhang, C.-R. Chang, Y. Ma, Y. Qu, Energy Environ. Sci. 2019, 12, 2298–2304.
- [21] J. Durst, A. Siebel, C. Simon, F. Hasché, J. Herranz, H. Gasteiger, Energy Environ. Sci. 2014, 7, 2255–2260.
- [22] H. Park, Y. Zhang, E. Lee, P. Shankhari, B. P. Fokwa, Chem-SusChem 2019, 12, 3726–3731.
- [23] a) E. Skúlason, G. S. Karlberg, J. Rossmeisl, T. Bligaard, J. Greeley, H. Jónsson, J. K. Nørskov, *Phys. Chem. Chem. Phys.* 2007, 9, 3241–3250; b) S. Gupta, M. K. Patel, A. Miotello, N. Patel, *Adv. Funct. Mater.* 2020, 30, 1906481; c) C. Tsai, K. Chan, J. K. Nørskov, F. Abild-Pedersen, *Surf. Sci.* 2015, 640, 133–140.
- [24] H. You, Z. Zhuo, X. Lu, Y. Liu, Y. Guo, W. Wang, H. Yang, X. Wu, H. Li, T. Zhai, CCS Chemistry 2019, 1, 396–406.

Manuscript received: February 14, 2022 Revised manuscript received: April 23, 2022 Accepted manuscript online: May 6, 2022